Selective deletion of the α5 subunit differentially affects somatic–dendritic *versus* axonally targeted nicotinic ACh receptors in mouse

Harald Fischer[1], Avi Orr-Urtreger[2], Lorna W. Role[3] and Sigismund Huck[1]

[1] *Division of Biochemistry and Molecular Biology, Centre for Brain Research, Medical University Vienna, Spitalgasse 4, A-1090 Vienna, Austria*
[2] *The Genetic Institute, Tel Aviv Sourasky Medical Center and Sackler School of Medicine, Tel Aviv University, 6 Weizmann Street, Tel Aviv 64239, Israel*
[3] *Center for Neurobiology and Behavior, College of Physicians and Surgeons, Columbia University, 722 West 168th Street, Research Annex Room 807, New York, NY 10032, USA*

We have compared the functional properties of nicotinic acetylcholine receptors (nAChRs) within both somatic and presynaptic domains of superior cervical ganglion (SCG) neurones from wild-type (WT) mice with those expressed by SCG neurones from mice with a targeted deletion of the gene for the α5-subunit. The functional profile of somatic nAChRs was assayed by direct macroscopic current recording and from measurements of nicotinic agonist-induced calcium transients with fura-2 imaging. The profile of nAChRs at presynaptic sites was assayed by measurement of nicotinic agonist-induced transmitter release (as preloaded [^{3}H]noradrenaline) under conditions of action potential blockade. We have examined the responses to the nicotinic agonists acetylcholine, nicotine, cytisine, dimethylphenylpiperazinium iodide (DMPP) and epibatidine. Macroscopic current and calcium imaging assays revealed several differences in the functional profile of somatic nAChRs in WT SCG neurones compared with those from mice with the α5 subunit deleted. Somatic nAChRs in control animals were more potently activated by cytisine as compared to DMPP. In contrast, DMPP was consistently more potent than cytisine in mice lacking the α5 nAChR subunit. Differences in the somatic nAChR rank order of potency were most prominent after a least 1 day *in vitro*. The magnitude of somatic nAChR responses to nicotinic agonists was not substantially different in control mice compared with those of α5 subunit-deleted animals. Comparison of presynaptic nAChR-mediated responses in WT *versus* α5 subunit-deleted animals revealed a very different set of changes in the functional profile of prejunctional nAChRs compared with somatic nAChRs. In contrast to somatic nAChRs, the responses of prejunctional receptors were markedly enhanced in α5 knockout animals compared with control. Furthermore, all prejunctional receptor responses were most potently activated by DMPP in both control and in α5 subunit-deleted mice. Hence, the presence or absence of the α5 subunit did not affect the rank order of potency of agonists at preterminal sites but greatly affected the magnitude of presynaptic nAChR-mediated responses. The enhanced efficacy of nicotine at presynaptic receptors was corroborated in an acute atrium preparation from postnatal α5 subunit-deleted mice. These results confirm and significantly extend our previous observation that in the sympathetic nervous system, somatic and prejunctional receptors are different and rely on the presence of the α5 subunit in a distinct manner.

(Received 22 September 2004; accepted after revision 14 December 2004; first published online 20 December 2004)
Corresponding author S. Huck: Division of Biochemistry and Molecular Biology, Centre for Brain Research, Medical University Vienna, Spitalgasse 4, A-1090 Vienna, Austria. Email: sigismund.huck@meduniwien.ac.at

Neuronal-type nicotinic acetylcholine receptors (nAChRs) play a pivotal role in trans-ganglionic signal transduction of the vegetative; nervous system (Wang *et al.* 2002*b*). The properties of these receptors have been studied extensively in the cholinergic (chick) ciliary ganglion (Williams *et al.* 1998; Conroy *et al.* 2000; Conroy *et al.* 2003), and in the chick (Yu & Role, 1998*a*,*b*; Devay *et al.* 1999) and rodent (Covernton *et al.* 1994; Silvilotti *et al.* 1997; Kristufek *et al.* 1999; Cuevas *et al.* 2000) sympathetic nervous system (for review see Skok, 2002).

The principal subunits that make up nAChRs in the vegetative nervous system are α3 and β4 (McGehee & Role, 1995; Skok, 2002). In heterologous expression

 DOI: 10.1113/jphysiol.2004.075788

systems these two subunits are sufficient to form functional receptors (reviewed by McGehee & Role, 1995). However, RT-PCR analysis, measurements of ligand binding, reported effects of α-bungarotoxin, and studies of subunit-specific antibodies indicate the presence of $\alpha5$, $\alpha7$, $\beta2$ and possibly $\alpha4$ subunits in rodent superior cervical ganglion (SCG) (Skok, 2002). The inclusion of $\alpha5$, $\alpha7$ and $\beta2$ nAChR subunits into ganglionic $\alpha3/\beta4$ pairs would be expected to change the functional profile of these receptors (Wang *et al.* 1996; Ramirez-Latorre *et al.* 1996; Groot-Kormelink *et al.* 1998; Gerzanich *et al.* 1998; Yu & Role, 1998*a*,*b*; Nelson & Lindstrom, 1999; Cuevas *et al.* 2000; Groot-Kormelink *et al.* 2001; Nelson *et al.* 2001; Nai *et al.* 2003).

Prior studies of the functional properties of nAChRs expressed by noradrenergic sympathetic or SCG neurones have primarily focused on receptors at somatic sites (Covernton *et al.* 1994; Mandelzys *et al.* 1995; Silvilotti *et al.* 1997; Yu & Role, 1998*a*,*b*). However, ganglionic neurones also have presynaptic (or prejunctional) nAChRs that are located on their axonal projections within the various target organs (Brain *et al.* 2001). Agonist-induced activation of these presynaptic nAChRs may generate antidromic volleys and cause the release of noradrenaline (Krauss *et al.* 1970).

We have previously shown (Kristufek *et al.* 1999) that prejunctional receptors are more sensitive to the nicotinic agonist 1,1-dimethyl-4-phenylpiperazinium iodide (DMPP), whereas somatic receptors in cultured rat SCG neurones are more potently activated by cytisine (Covernton *et al.* 1994; Kristufek *et al.* 1999). The distinct pharmacological profiles of somatic *versus* presynaptic nAChRs indicates fundamental differences in these receptor populations that may be due, at least in part, to differences in the subunit composition of the receptors (McGehee & Role, 1995; Nai *et al.* 2003). Attempts to dissect the subunit composition of these distinct receptors by comparing the properties of native receptors with receptors of defined composition expressed in heterologous systems have been less than successful in assigning a particular set of subunits that correspond to the functional profiles of rat SCG nAChRs (Covernton *et al.* 1994; Silvilotti *et al.* 1997; Lewis *et al.* 1997).

We have chosen a somewhat different tactic to the analysis of native subunit composition, examining the 'pharmacological fingerprints' (Covernton *et al.* 1994; Kristufek *et al.* 1999) of both somatic and prejunctional nAChRs in neurones from mice with functional deletions of a particular subunit (Champtiaux & Changeux, 2004). This report, as first part in a series of experiments, deals with studies on nicotinic receptors in the SCG from mice with a targeted deletion of the $\alpha5$ subunit (Wang *et al.* 2002*a*,*b*, 2004; Salas *et al.* 2003). The general behaviour and gross anatomy of $\alpha5$ knockout mice are similar to their wild-type littermates (reviewed by Wang *et al.* 2002*b*). However, $\alpha5$ knockout mice are, for example less susceptible to nicotine-induced seizure (Kedmi *et al.* 2004), have more severe symptoms in experimental colitis (A. Orr-Urtreger, manuscript in preparation), and show an altered cardiac parasympathetic ganglionic transmission (Wang *et al.* 2002*a*). For a better understanding of the role of the $\alpha5$ subunit in ganglionic transmission, the effects of $\alpha5$ deletion now presented encourage one to take a second look for specific effects of nicotine in such mice.

Methods

Animals

Experiments were performed on cell cultures of dispersed SCG neurones or on acute atrial preparations taken from early postnatal mice with $\alpha5$ subunit deficiency ($\alpha5$ −/−) on C57BL/6J background and their wild-type ($\alpha5$+/+) littermates (Salas *et al.* 2003).

Cell culture

Superior cervical ganglia were dissected from 4- to 6-day-old mouse pups humanely killed, as required by the Guidelines of the Animal Care Committee, by decapitation. The ganglia were dispersed to single cells, and plated as previously described (Boehm & Huck, 1995). Briefly, ganglia were freed from adhering connective tissue and blood vessels and incubated in a combination of collagenase IA (0.5 mg ml^{-1}, Sigma) and dispase (1.0 mg ml^{-1}, Roche Applied Science) for 20 min at 36.5°C. Subsequently, the ganglia were rinsed three times in Ca^{2+}-free Tyrode solution and trypsinized (0.25% trypsin in Tyrode solution; Worthington) for 15 min at 36.5°C and dispersed by trituration in culture medium. Dispersed neurones were plated either onto 5-mm discs punched out of tissue culture dishes (Nunc) for experiments measuring transmitter release, or onto glass coverslips (Assistent) for patch-clamp recordings and fura-2 spectrofluorometry. Glass coverslips were treated by submersion in concentrated nitric acid for 2 days and thorough rinses thereafter with distilled water. Tissue culture discs and cleaned glass coverslips were coated with poly L-ornithine (100 mg (l H_2O)$^{-1}$; Sigma), followed by 250 μl laminin (Becton Dickinson; dissolved as 0.01 g l^{-1} in Neurobasal A medium, Gibco-Invitrogen). Approximately, 7500 cells were seeded into glass rings of 6 mm (release experiments) or 8 mm (patch clamp and calcium imaging) in order to confine them to the disc or the centre of the coverslip.

The culture medium consisted of Neurobasal A medium, supplemented with the B-27 additive (20 ml l^{-1}; Gibco-Invitrogen), 25000 IU l^{-1} penicillin, 25 mg l^{-1} streptomycin (Gibco-Invitrogen), 0.5 mM L-glutamine

(Sigma) and 20–50 $\mu g\,l^{-1}$ nerve growth factor (NGF; R & D Systems).

Cultures meant for release experiments were maintained in the presence of 5% fetal bovine serum (Gibco-Invitrogen) and in 5% CO_2, whereas the serum-free cultures used for calcium imaging and patch-clamp recordings were kept in 7% CO_2.

Spectrofluorometry: fura-2 calcium imaging

Measurements of intracellular Ca^{2+} concentrations were performed at room temperature on an inverted Nikon Diaphot 300 microscope connected to a spectrofluorometrical calcium imaging system (VisiTech, Sunderland, UK). Cells on glass coverslips were 'loaded' with dye by incubation in culture medium including 5 μM acetoxymethyl ester form of fura-2 (fura-2 AM Molecular Probes). Preparations were rinsed twice with bathing solution prior to transfer to a recording chamber. The bathing (external) solution used for both calcium imaging and for patch-clamp analysis contained (mM): NaCl 120, KCl 3.0, $CaCl_2$ 2.0, $MgCl_2$ 2.0, glucose 20 and Hepes 10; adjusted to pH 7.3 with NaOH, and a final osmolarity of 280 mosmol l^{-1}.

Changes in intracellular Ca^{2+} concentrations were determined by dual excitation at 340 and 380 nm, and by measuring emission at 510 nm. Measured F_{340}/F_{380} ratios were transformed into Ca^{2+} concentration by the eqn (1) of Grynkiewicz (Grynkiewicz *et al.* 1985):

$$[Ca^{2+}] = K_{eff}(R - R_{min})/(R_{max} - R) \qquad (1)$$

where $R_{min} = Sf_1/Sf_2$; $R_{max} = Sb_1/Sb_2$; $K_{eff} = K_D \times Sf_2/Sb_2$. $[Ca^{2+}]$ is the calculated calcium concentration; R_{min} the calibration constant for F_{340}/F_{380} ratio at zero free calcium; R_{max} the calibration constant F_{340}/F_{380} ratio for 39.8 μM free calcium; R the actually measured F_{340}/F_{380} ratio; Sf_1 the F_{340} determined by calibration with zero free calcium buffer; Sf_2 the F_{380} determined by calibration with zero free calcium buffer; Sb_1 the F_{340} determined by calibration with 39.8 μM free calcium buffer; Sb_2 the F_{380} determined by calibration with 39.8 μM free calcium buffer; K_{eff} the calibration constant; and K_D the dissociation constant for fura-2 (224 nM at room temperature Grynkiewicz *et al.* 1985). The K_{eff}, R_{min} and R_{max} calibration constants were determined for a given setting by measuring fura-2 fluorescence intensities in the absence or presence of 39.8 μM free calcium (Calcium Calibration Set, Molecular Probes).

Excitation light from a monochromatic fluorescent light source (QuantiCell FSM900, VisiTech) was directed to the sample via an appropriate filter set (Omega). Images were taken with a Nikon Fluor 40x/1.3 Ph4DL oil immersion objective and an intensified CCD camera (Stanford Photonics XR/Mega10 GEN III+). Registration of F_{340}/F_{380} ratio images was at 1 Hz and controlled by the QuantiCell 2000 software (version 2.0e; VisiTech). We determined the Ca^{2+} concentrations in single cells off-line by selecting areas of interest from images recorded while applying our test substances. The effects of drugs were assessed by calculating the peak increase in intracellular calcium from baseline values. Nicotinic agonists were dissolved in recording buffer and applied in the presence of 0.5 μM tetrodotoxin (TTX, Latoxan) by a superfusion device (DAD-12, Adams & List) at a rate of one concentration per minute. Application times were adjusted to the occurrence of peak effects (12 s for low concentrations, 6 s for high concentrations of agonists).

Simultaneous calcium imaging and perforated-patch voltage-clamp recordings

Neurones loaded with fura-2 AM as described above were also assayed by electrophysiological recordings using perforated patch-clamp techniques (Rae *et al.* 1991). The recording pipettes had tip resistances of 1.5–3 MΩ when filled with 200 $\mu g\,ml^{-1}$ amphotericin B (Sigma A-4888) in a standard internal solution containing (mM): K_2SO_4 75, KCl 55, $MgCl_2$ 8, Hepes 10, adjusted to pH 7.3 with (KOH). Cells were voltage clamped at −70 mV. For signal processing we used an Axopatch 200A (Axon Instruments) patch-clamp amplifier, a Digidata 1200 (Axon Instruments) A/D converter, and the pCLAMP 8 software (Axon Instruments).

[^{3}H]Noradrenaline uptake and superfusion

The techniques for loading cultures with [^{3}H]noradrenaline (NA) and subsequent superfusion for measurement of [^{3}H]NA release were as previously described (Kristufek *et al.* 1999). Briefly, the cultures were incubated with 0.03 μM [^{3}H]NA in culture medium containing 1 mM ascorbic acid for 60 min at 36.5°C. Culture discs were then transferred to low-volume chambers and superfused at 25°C with buffer containing (mM): NaCl 120, KCl 3, $CaCl_2$ 2, $MgCl_2$ 2, glucose 20, Hepes 10, fumaric acid 0.5, sodium pyruvate 5.0 and ascorbic acid 0.57; adjusted to pH 7.4 with NaOH. The rate of superfusion was 1 ml min^{-1}, and superfusate was collected in 4-min samples before a 60-min washout period. Residual radioactivity within preparations after the release procedures was determined by extracting cultures at the end of an experiment with 1% sodium dodecyl sulphate (SDS). Radioactivity in extracts and collected fractions was determined by liquid scintillation counting.

Stimulation-induced radioactive outflow was achieved by adding nicotinic agonists to the superfusion medium for 15 s. Cultures were challenged with a first stimulus (S1) 12 min after the washout period (i.e. 72 min

after initiation of superfusion) and to a maximum of three additional stimuli (S2, S3 and S4) at 20 min intervals. Concentration–response relationships for nicotinic agonists were established by a measuring a maximum of four stimuli with increasing concentrations of the agents in the absence or continuous presence of 0.25 μM TTX.

Mouse atria were taken from 6-day-old pups killed by decapitation and collected in ice-cold superfusion buffer containing (mM): NaCl 118, KCl 4.8, $CaCl_2$ 2.5, $MgSO_4$ 1.2, $NaHCO_3$ 25, KH_2PO_4 1.2, Na_2-EDTA 0.03, glucose 11, ascorbic acid 0.57, fumaric acid 0.5 and sodium pyruvate 5.0; and bubbled with 95%O_2–5%CO_2. Loading of radioactivity was achieved by adding 0.03 μM [^{3}H]NA and 1 mM ascorbic acid to superfusion buffer and incubating atria for 60 min at 36.5°C. One intact atrium was placed thereafter into each chamber and rinsed with superfusion buffer for 60 min before samples were collected at 4 min intervals. In order to block monocemine oxidase A (MAO_A) activity and thus reduce the basal outflow of radioactivity, atria were exposed to 0.5 μM clorgyline for 20 min during the initial washout period (Kristufek *et al.* 2002). Stimulation-induced outflow of [^{3}H]NA was achieved by either electrical field stimulation (120 monophasic pulses delivered at 3 Hz, 0.5 ms, 50 V cm^{-1}, 40 mA), or by adding 100 μM nicotine (in the presence of 0.5 μM TTX) for 15 s to the superfusion buffer. Residual radioactivity was determined by extracting atria at the end of an experiment with 1% SDS and sonication.

Calculation of basal and stimulation-evoked [^{3}H]NA outflow

Rates of [^{3}H]NA outflow were obtained by dividing the amount of [^{3}H]NA collected during a 4-min period by the total [^{3}H]NA content of cultures at the beginning of the corresponding 4-min collection period (expressed as fractional rate). Basal outflow before the first stimulus (i.e. the basal fractional rate) was termed L1. Stimulation-evoked outflow was calculated as the difference between the total [^{3}H]NA outflow during and after stimulation on the one hand, and the estimated basal outflow on the other hand, assuming that basal release follows a linear decline (Kristufek *et al.* 1999). The (stimulus-induced) difference was expressed as a percentage of the total radioactivity in the cultures at the beginning of the respective stimulation (S%, see Kristufek *et al.* 1999).

Calculation of concentration–response curves and potency ratios

All data are presented as arithmetic means ± S.E.M. The significance of differences was evaluated by means of the unpaired Student's *t*-test, unless indicated otherwise. Raw data from fura-2 imaging, patch-clamp recordings, and transmitter release experiments were converted into concentration–response curves using self-written script files for SigmaPlot 2000 (SPSS Inc.). Full concentration–response curves for agonists were fitted by unweighted non-linear regression to the logistic equation:

$$E_x = E_{max} x^p / \left(EC_{50}{}^p + x^p\right) \quad (2)$$

where E_x is the response to a certain agonist concentration; x the arithmetic dose; E_{max} the maximal response; p a slope factor; and EC_{50} the dose that gives a half-maximal response. Computation utilized either SigmaPlot 2000 (SPSS Inc.) or the ALLFIT program (DeLean *et al.* 1978). The ALLFIT program calculates parameter estimates for EC_{50} values, the slope p (which is numerically identical to the Hill coefficient, see DeLean *et al.* 1978), and E_{max}, as well as appropriate standard errors and leaves the option to fit curves with or without shared parameters by non-linear regression. The program uses F statistics as the 'extra sum of squares' introduced when testing for independent *versus* shared parameters of two curves.

Low-concentration potency ratios were determined according to Covernton *et al.* (Covernton *et al.* 1994; Kristufek *et al.* 1999). Hence, dose–response curves (at the low-concentration end) were fitted simultaneously by non-linear regression with logistic equations that were constrained to be parallel (i.e. with a shared slope parameter, p). The maximum response was fixed to values deduced from full-range concentration–response curves of previous experiments. Adequacy of the fits was judged by eye (e.g. see Figs 2 and 8).

Materials

Materials and reagents were obtained as noted and from the following sources: (−)-[ring-2,5,6 ^{3}H]noradrenaline (56.9 Ci mmol^{-1}, NEN); acetylcholine chloride (ACh), 1,1,-dimethyl-4-phenylpiperazinium iodide (DMPP) cytisine, epibatidine and clorgyline hydrochloride from Sigma; and all other chemicals were from Merck (analytical grade).

Results

In the current series of experiments we established pharmacological fingerprints of somatic and prejunctional receptors in cultured SCG neurones by comparing the responses to five established nicotinic agonists: nicotine, cytisine, DMPP, ACh and epibatidine. Due to the relatively high calcium permeability of neuronal-type nAChRs, as compared with their muscle nAChR cousins (reviewed by McGehee & Role, 1995), the properties of receptors at somatic sites could also be assessed by spectrofluorometry using the Ca^{2+}-sensitive dye, fura-2, in addition to patch-clamp recording. As in our previous study (Kristufek *et al.* 1999), functions of prejunctional receptors were monitored by measuring the outflow of

preloaded [^{3}H]NA as a result of calcium influx at sites of transmitter release. Generation of action potentials, and ensuing calcium entry through voltage-gated calcium channels, was prevented by adding TTX to the buffer solutions. We have shown previously that under these conditions, nicotinic agonists are unable to depolarize SCG varicosities sufficient for an activation of high voltage-activated calcium channels (Kristufek *et al.* 1999).

Somatic nAChRs: assessment of function by full concentration–response curves of nicotinic agonists and differences in rank order of potency between α5 (+/+) and α5 (−/−) mice

An assessment of potencies of nicotinic agonists by calcium imaging using fura-2, and deduced from full concentration–response curves in α5 (+/+) mouse SCG neurones after 4–5 days *in vitro* (DIV) (4/5 DIV) produced results very similar to patch-clamp observations previously made in the rat SCG (Covernton *et al.* 1994; Kristufek *et al.* 1999). Hence, out of the four classical agonists, cytisine was most potent to activate somatic receptors, followed by DMPP, nicotine and ACh (in the presence of 0.1 μM atropine; Fig. 1; Table 1). Potency ratios calculated from EC_{50} values (Table 1) relative to the standard cytisine (1.0) were 0.80 (DMPP), 0.64 (nicotine) and 0.26 (ACh). These values are strikingly close to those obtained in rat (DMPP, 0.62; nicotine, 0.60; Ach, 0.34; all relative to cytisine Kristufek *et al.* 1999). In all assays presented in our present study, the potency of epibatidine exceeded the most potent concurrent nicotinic agonist by at least three orders of magnitude (Figs 1 and 7, and Table 1 and 2).

With one notable exception, cytisine, the EC_{50} values for the activation of somatic receptors were not substantially different in α5 (+/+) and α5 (−/−) mice (Fig. 1; Table 1). Cytisine was about 1.6 times less potent in the α5 (−/−) mice compared with α5 (+/+) controls (Fig. 1; Tables 1, $P < 0.01$). This shift of potency was sufficiently large to change the rank order of agonist potency in the α5 (−/−) animals to DMPP (1.50), followed by cytisine (1.0), nicotine (1.00) and ACh (0.42).

In addition to the significant effects on rank order of agonist potency, there was a trend towards increased efficacy of a subset of the nicotinic agonists, as assessed from the magnitude of the somatic responses in α5 (−/−) *versus* α5 (+/+)-derived neurones (Fig. 1*F*). Thus, the maximum increases in calcium measured in α5 (−/−) animals were significantly larger in response to cytisine ($P < 0.05$), DMPP ($P < 0.01$) and epibatidine ($P < 0.05$) but did not differ significantly for nicotine and ACh (Fig. 1*F*). The trend towards a higher maximum responses was also apparent in analyses of data pooled for all agonists (Fig. 1*F*, overall). Hence, in α5 (−/−) mice, the maximum increase of calcium in response to the agonists exceeded the effects in α5 (+/+) mice by a factor of 1.14 ($P < 0.01$, $n = 113$ and 123 for α5 (+/+) and α5 (−/−) mice, respectively).

Table 1. Enhancement of somatic calcium by saturating concentrations of nicotinic agonists: comparison between α5 (+/+) and α5 (−/−) mice

Agonist		EC_{50} (μM)	Slope	*n*
DMPP	α5 (+/+)	11.47 ± 0.71	2.20 ± 0.21	20
DMPP	α5 (−/−)	9.92 ± 0.43**	2.32 ± 0.19	24
Cytisine	α5 (+/+)	9.27 ± 0.18	1.62 ± 0.04	26
Cytisine	α5 (−/−)	14.95 ± 0.47**	1.98 ± 0.10	30
Nicotine	α5 (+/+)	14.27 ± 1.09	2.14 ± 0.24	27
Nicotine	α5 (−/−)	14.87 ± 1.17$^{n.s.}$	2.15 ± 0.25	27
ACh	α5 (+/+)	34.16 ± 2.55	1.91 ± 0.20	20
ACh	α5 (−/−)	35.40 ± 2.01$^{n.s.}$	2.09 ± 0.18	22
Epibatidine	α5 (+/+)	0.0057 ± 0.0002	2.86 ± 0.20	20
Epibatidine	α5 (−/−)	0.0062 ± 0.0001**	2.81 ± 0.03	20

EC_{50} values, slope, and number of cells (*n*) for the agonist-induced enhancement of intracellular calcium, measured in SCG neurones from α5 (+/+) and α5 (−/−) mice after 4–5 DIV. Data are means ± S.E.M. Parameters were determined by fitting normalized data points of cells as shown in Fig. 1 with eqn (2). EC_{50} values differed between α5 (+/+) and α5 (−/−) mice for agonists where indicated (**$P < 0.01$). Note that cytisine is more potent by a factor of 1.61 in α5 (+/+) than in α5 (−/−) mice.

Somatic nAChRs: assessment of function by low concentration potency ratios confirms results of full concentration–response curves

Estimates of EC_{50} values when deduced from full concentration–response curves may be misleading (Covernton *et al.* 1994; Kristufek *et al.* 1999). Therefore, we used an additional approach to compare the potencies of our four standard agonists at concentrations not exceeding EC_{50} values ('low-concentration potency ratios', see Covernton *et al.* 1994). This approach minimizes the contribution of receptor desensitization seen at high concentration of agonists and eliminates 'between neurone' variance as comparative measurements of potency ratios can be done on the same cells (Figs 2 and 3). Potency ratios determined from individual neurones could then be pooled for calculation of the statistics (Fig. 4).

Potency ratios determined at lower agonist doses confirmed our findings on the differences in rank order potency and potency ratios of neurones from α5 (+/+) *versus* α5 (−/−) mice, as deduced from the EC_{50} values. Hence, in SCG neurones of α5 (+/+) mice, cytisine was the most potent agonist, followed by DMPP and nicotine, and then ACh (1, 0.67 ± 0.02, 0.68 ± 0.03 and 0.51 ± 0.02, respectively; means ± S.E.M., $n = 21$ from four different preparations; see Fig. 4*A*, data points at 4 DIV). In contrast, examination of SCG neurones from α5 (−/−) mice revealed the distinct rank order

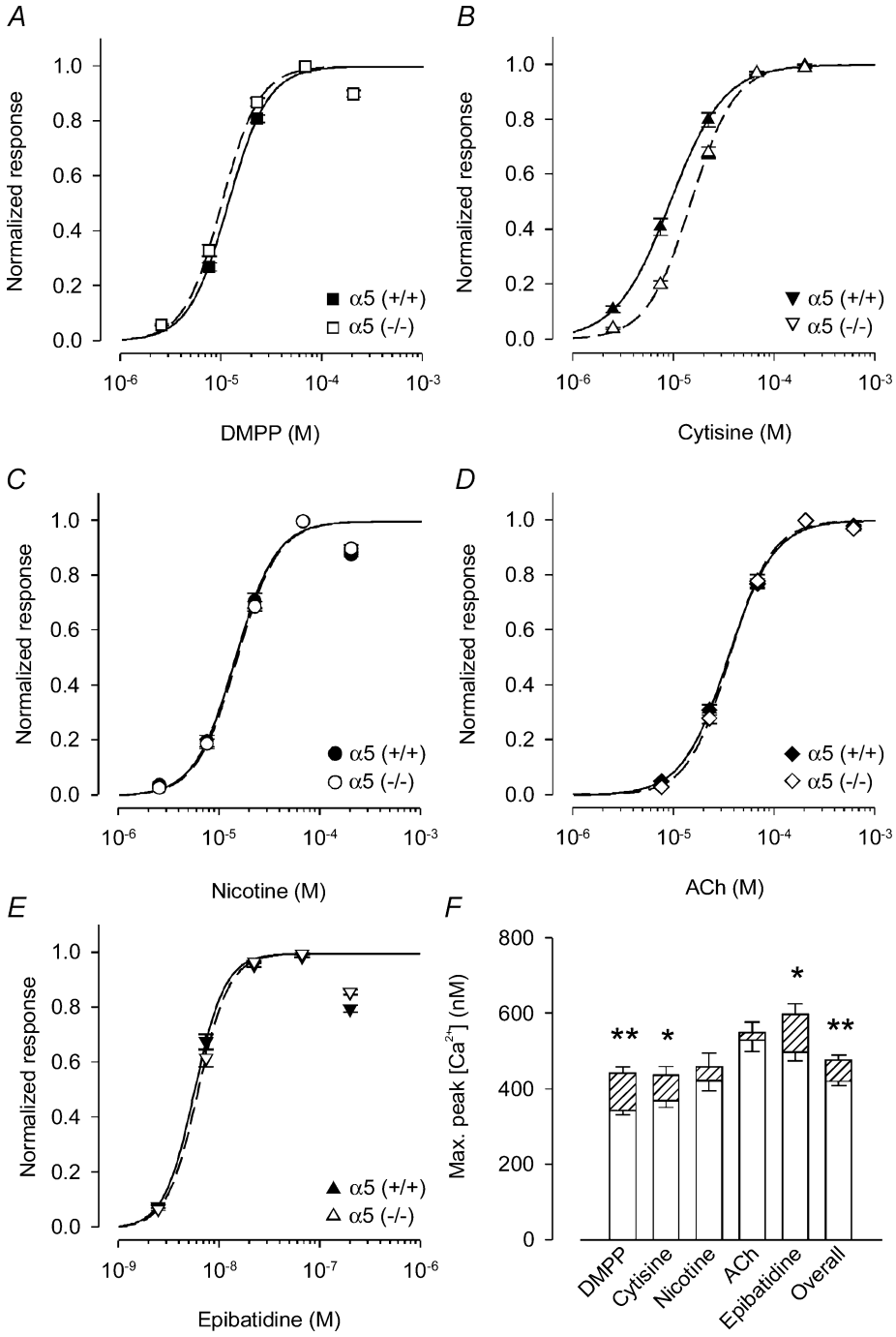

Figure 1. Enhancement of somatic calcium signalling response to nicotinic agonists: comparison between α5 (+/+) and α5 (−/−) mice

A–E, calcium transients in the soma region were recorded by fura-2 calcium imaging in response to DMPP (*A*), cytisine (*B*), nicotine (*C*), ACh (in the presence of 0.1 μM atropine, *D*) and epibatidine (*E*). Recordings were done in the presence of 0.5 μM TTX. Full concentration–response curves for each of the agonists were determined in at least 20 neuronal somata of two to three different preparations of control or of α5 (−/−) neurones (4–5 DIV). Values of individual cells were normalized with respect to the concentrations yielding maximum response (DMPP and nicotine, 67 μM; cytisine and Ach, 200 μM; epibatidine, 67 nM), and then fitted for determination of EC_{50} values using eqn (2). Results from α5 (+/+) animals are indicated by filled symbols and continuous lines, those from α5 (−/−) by open symbols and dashed lines. Fitted parameters are summarized in Table 1. There were only minor differences in EC_{50} values between genotypes with the exception of cytisine. Cytisine was more potent in α5 (+/+) as compared to α5 (−/−) mice (EC_{50}: α5 (+/+), 9.27 ± 0.18 μM; α5 (−/−), 14.95 ± 0.47 μM; $P < 0.01$). *F*, maximum calcium signal for each agonist at somatic nAChRs obtained by fitting the dose–response to

Table 2. Transmitter release in response to activation of prejunctional nicotinic acetylcholine receptors: comparison between α5 (+/+) and α5 (−/−) mice

Agonist		EC_{50} (μM)	Slope	*n*
DMPP	α5 (+/+)	35.15 ± 1.87	3.63 ± 0.82	12
DMPP	α5 (−/−)	25.45 ± 0.98**	3.62 ± 0.47$^{n.s.}$	21
Cytisine	α5 (+/+)	56.64 ± 5.76	2.06 ± 0.44	23
Cytisine	α5 (−/−)	46.94 ± 2.78$^{n.s.}$	3.05 ± 0.56$^{n.s.}$	36
Nicotine	α5 (+/+)	34.44 ± 1.43	8.84 ± 2.61	18
Nicotine	α5 (−/−)	29.44 ± 1.12*	4.33 ± 0.70$^{n.s.}$	27
ACh	α5 (+/+)	197.46 ± 11.09	2.72 ± 0.44	21
ACh	α5 (−/−)	98.89 ± 3.82**	4.13 ± 0.53*	31
Epibatidine	α5 (+/+)	0.0387 ± 0.0024	4.57 ± 1.17	14
Epibatidine	α5 (−/−)	0.0282 ± 0.0014**	3.33 ± 0.52$^{n.s.}$	19

EC_{50} values, slope and number of individual culture discs (*n*) for TTX-insensitive, agonist-induced transmitter overflow in α5 (+/+) and α5 (−/−) mice. Parameters were determined by fitting normalized data points of cultures in triplicate as shown in Fig. 7 with eqn (2). Data are means ± S.E.M.; *n*, normalized data points of cultures in triplicate, derived from three (DMPP tested at α5(+/+)) to nine (cytisine and ACh tested at α5(−/−)) experiments each. Note that in both α5 (+/+) and α5 (−/−) mice, DMPP is more potent at inducing transmitter release than cytisine (by a factor of 1.61 and 1.84, respectively). EC_{50} values and slope factors differed between α5 (+/+) and α5 (−/−) mice for agonists where indicated (**$P < 0.01$, *$P < 0.05$, *F* test).

potency of DMPP > cytisine > nicotine > > ACh. Thus direct assessment of low-concentration potency ratios (cytisine, 1; DMPP, 1.34 ± 0.02; nicotine, 0.90 ± 0.01; Ach, 0.30 ± 0.01; means ± S.E.M., $n = 16$ out of three different preparations; see Fig. 4*B*, data points at 4 DIV) confirms the results obtained from full dose–response curves.

Simultaneous fura-2 calcium imaging and patch-clamp recordings in the same cell further confirmed the differences of somatic nAChRs agonist potency ratios between α5 (+/+) and α5 (−/−) mice. Both techniques yielded identical potency ratios in within genotype comparisons of either α5 (+/+) or α5 (−/−) mice (compare Figs 2 and 3). It is notable that the time course of calcium transients was much slower than the evoked currents recorded in response to application of agonists. In addition we noted a trend towards higher magnitude changes in DMPP-evoked Ca^{2+} signalling in neurones from α5 subunit-deleted mice (compare Figs 2 and 3).

Potency ratios are affected by the age of cultures in α5 (+/+) mice, but not in α5 (−/−) mice

All observations presented so far were made on mouse SCG neurones maintained in culture for 4–5 days. However, the subunit composition of nAChRs changes with the age of cultures (De Koninck & Cooper, 1995). We therefore wanted to know whether these changes were paralleled by an adjustment of potency ratios. It is striking that cytisine has an exceedingly high potency compared to the other agonists when tested after 1 DIV in SCG neurones from α5 (+/+) mice (potency ratio of DMPP compared to cytisine, 0.30 ± 0.02, means ± S.E.M.; $n = 6$ of two preparations, Fig. 4*A*). By 4 DIV, the ratio declined to 0.67 ± 0.02 ($n = 21$ of four preparations, see above), and after 6 DIV, DMPP and cytisine were almost equipotent in neurones from α5 (+/+) mice (cytisine, 1; DMPP, 0.95 ± 0.01, $n = 7$ of two preparations; difference to 1 DIV significant at $P < 0.01$). The changes in the potency of nicotine and ACh initially followed the time course of DMPP, but then declined relative to DMPP after 9 and 12 DIV (Fig. 4*A*).

In contrast to the developmental changes in somatic responses in α5 (+/+) animals, somatic nAChRs of α5 (−/−) mice remained about constant throughout the incubation period. DMPP was more potent than cytisine at all points examined (potency ratio after 1 DIV, 1.39 ± 0.01; $n = 6$ of two preparations, Fig. 4*B*). Hence, the α5 genotypes were most distinct at 1 DIV, when potency ratios between DMPP and cytisine differed by the quotient 1.39/0.30 (i.e. 4.63). Overall, these data are consistent with changes in the nAChR composition with *in vitro* development of α5 (+/+) neurones that does not occur when the α5 subunit is absent.

TTX-sensitive *versus* TTX-insensitive transmitter release

Experiments delineated above assess the pharmacological fingerprints of somatic nAChRs in SCG neurones from both α5 (+/+) and α5 (−/−) mice. Our next task was to apply a similar analysis to determine the functional profile of the presynaptic receptor pools. As detailed in a previous study (Kristufek *et al.* 1999), the function of prejunctional receptors was monitored indirectly by measuring the outflow of preloaded [^{3}H]NA in response to nicotinic

eqn (2) without prior normalization. Open columns are results from α5 (+/+) mice, hatched columns are the surplus of responses as seen in α5 (−/−) animals. All agonists show a tendency towards higher efficacy in the α5 (−/−) responses, although the difference is only significant for DMPP (344 ± 11 nM *versus* 443 ± 17 nM; $n = 20$ and 24 for α5 (+/+) and α5 (−/−) mice, respectively; $P < 0.01$), epibatidine (499 ± 24 nM *versus* 599 ± 28 nM; $n = 20$ for both α5 (+/+) and α5 (−/−); $P < 0.05$) and cytisine (370 ± 17 nM *versus* 438 ± 23 nM; $n = 26$ and 30 for α5 (+/+) and α5 (−/−); $P < 0.05$). Maximal effects of ACh in α5 (+/+) animals (530 ± 29 nM; $n = 20$) were significantly larger than effects of DMPP ($P < 0.01$), cytisine ($P < 0.01$), and nicotine ($P < 0.05$). In α5 (−/−) animals, the maximal effects of ACh (551 ± 27 nM; $n = 22$) significantly exceeded those of DMPP and cytisine ($P < 0.01$).

agonists. The component of transmitter outflow that remains upon stimulation with nicotine in the presence of TTX ('TTX-insensitive transmitter release') thus reflects the function of presynaptic receptors (Kristufek *et al.* 1999). Subtraction of this component from overall release (i.e. in the absence of TTX) reveals the 'TTX-sensitive component'.

We first examined whether SCG neurones from mice, like those from rat, have both the TTX-sensitive as well as the TTX-insensitive component. Results from these experiments for both $\alpha5$ (+/+) and $\alpha5$ (−/−) animals are shown in Fig. 5. Curve fits of data points by eqn (2) yielded identical EC_{50} values for the TTX-insensitive component of nicotine-induced transmitter outflow in $\alpha5$ (+/+) and $\alpha5$ (−/−) mice ($\alpha5$ (+/+), 37.46 μM; $\alpha5$ (−/−), 37.04 μM, Fig. 5). Note, however, that the maximum of the TTX-insensitive component was strikingly different between $\alpha5$ (−/−) and $\alpha5$ (+/+) mice. As shown in more detail below (Fig. 7), TTX-insensitive transmitter release was significantly enhanced in $\alpha5$ (−/−) mice not only in response to nicotine, but also by the other agonists tested.

TTX-sensitive release was induced with an EC_{50} of 15.82 μM in $\alpha5$ (+/+) and an EC_{50} of 11.71 μM in $\alpha5$ (−/−) mice (Fig. 5*A2* and *B2*) and thus appeared to be more potently activated in animals lacking the $\alpha5$ subunit. A plausible explanation for the higher potency of nicotine in inducing TTX-sensitive release in $\alpha5$ (−/−) mice might be a higher efficacy of the agonists on nAChRs assembled without the contribution of $\alpha5$ subunits. If this were the case, and assuming that neither

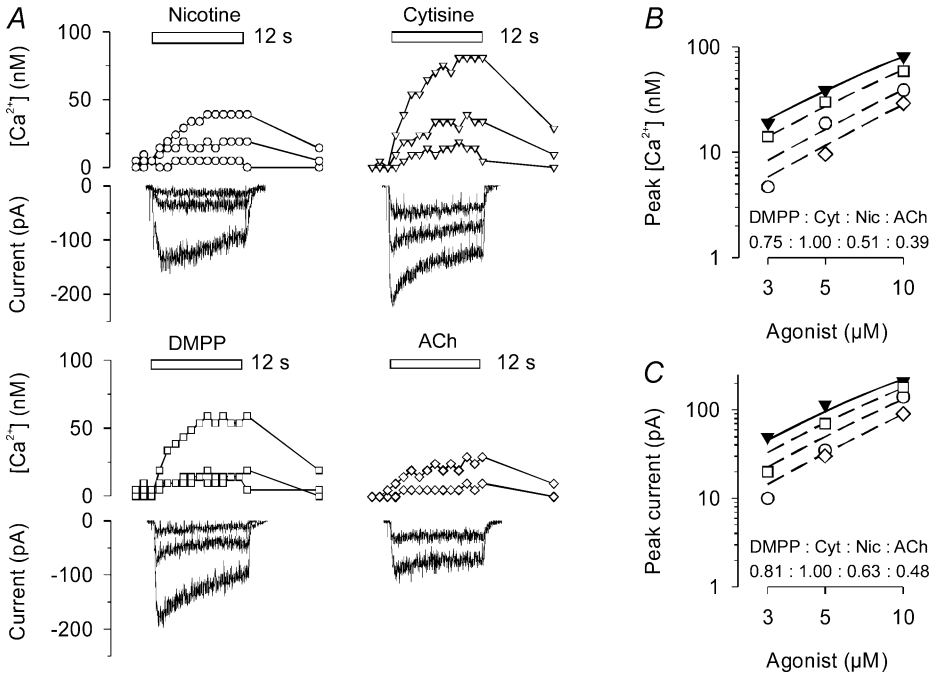

Figure 2. Agonist-induced calcium transients and whole cell currents measured in $\alpha5$ (+/+) SCG neurone
Examples are shown from one of the three $\alpha5$ (+/+) neurones successfully assayed with both calcium imaging and whole cell current recording to assess the effects of agonist at the low end of the concentration–response curve. *A*, calcium transients, concurrently determined with whole-cell currents, in response to 12-s applications (indicated by bars) of nicotine, cytisine, DMPP or ACh (in the presence of 0.1 μM atropine). Concentrations were 3, 5 and 10 μM (nicotine, cytisine and DMPP, respectively), and 5 and 10 μM (ACh). Sharp deviations in current traces are due to the CCD camera shutter. The experiment was conducted on a 4 DIV preparation. *B*, dose–response relationship of peak calcium transients constructed from original recordings as shown in *A*. Data are mean peak transients measured in duplicate for each agonist. Curves based on eqn (2) were simultaneously fitted to data points by unweighted non-linear regression using the Allfit routine with the constraint of a shared slope and a fixed maximum as described in Methods. Filled inverted triangles and continuous line show the concentration–response curve for cytisine (Cyt); dashed lines and open symbols are effects of DMPP (□), nicotine (Nic, ○) and ACh (◇). Potency ratios relative to cytisine (1.0) were 0.75 (DMPP), 0.51 (nicotine) and 0.39 (ACh). *C*, dose–response relationship of peak currents constructed from original recordings as shown in panel *A*. Data are mean peak transients measured in duplicate for each agonist. Curves based on eqn (2) were simultaneously fitted to data points by unweighted non-linear regression using the Allfit routine with the constraint of a shared slope and a fixed maximum as described in Methods. Filled inverted triangles and continuous line show the concentration–response curve for cytisine; dashed lines and open symbols are effects of DMPP (□), nicotine (○) and ACh (◇). Potency ratios relative to cytisine (1.0) were 0.81 (DMPP), 0.63 (nicotine) and 0.48 (ACh).

the properties or distribution of voltage-gated sodium channels are affected by the α5 subunit genotype, a lower concentration of nicotine might suffice to depolarize neurones to the threshold level for the activation of sodium channels. We tested this hypothesis by exploring transmitter release upon exposure of cultures to low concentrations of nicotine in the presence and absence of TTX (Fig. 5*A3* and *B3*). Our experiments revealed that the TTX-sensitive component reached about the same maximum in both α5 (+/+) and α5 (−/−) mice. However, maximal effects were obtained with 10 μM nicotine in α5 (−/−) animals, whereas it took about 30 μM of nicotine in α5 (+/+) mice (Fig. 5*A3* and *B3*).

These observations are compatible with the idea that nAChRs assembled in α5 (−/−) mice are activated more efficaciously by nicotine than those in α5 (+/+) controls. Note that release measured in all cases is entirely dependent on the presence of calcium in the superfusion buffer even in α5 (−/−) animals, where the TTX-insensitive component of nicotine-induced transmitter release is markedly enhanced relative to control (Fig. 6). On average, 100 μM nicotine causes a 22.8 ± 4.1% ($n = 24$) depletion of radioactivity in cultures after 2 DIV (see Fig. 9).

Prejunctional nAChRs: assessment of function by full concentration–response curves of nicotinic agonists in α5 (+/+) and α5 (−/−) mice

Having assessed the basic properties of TTX-sensitive and TTX-insensitive transmitter release in both α5 (+/+) and α5 (−/−) mice we next examined the pharmacological profile of the prejunctional nAChRs in the α5 (+/+) and α5 (−/−) animals in more detail. EC_{50} values deduced from full concentration–response curves indicate a lower potency of DMPP and ACh, but not of nicotine or cytisine, in α5 (+/+) mice (Fig. 7; Table 2) as compared to the rat

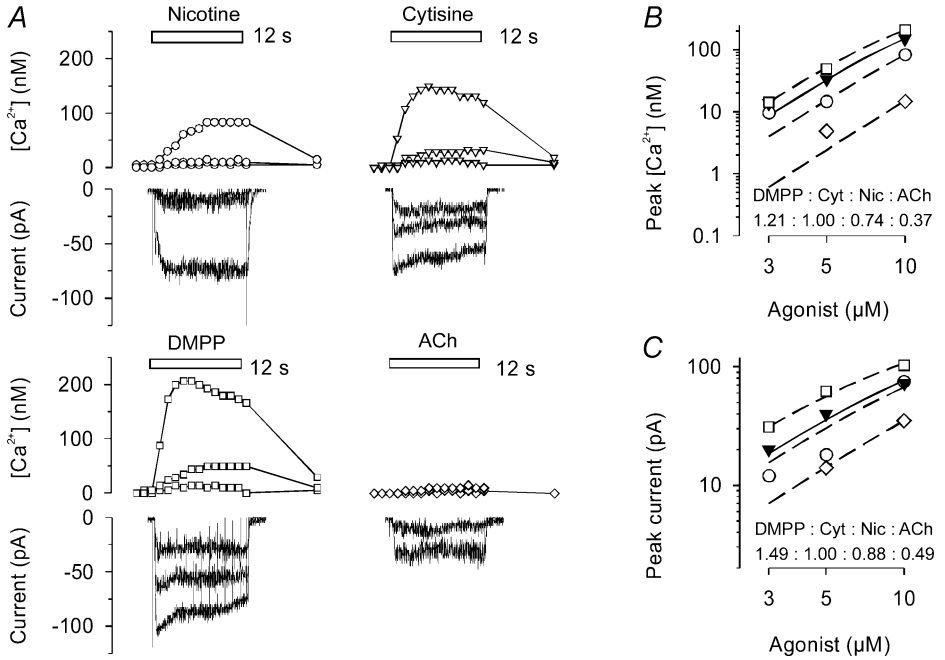

Figure 3. Agonist-induced calcium transients and whole cell currents measured in α5 (−/−) SCG neurone
Examples are shown from one of the three α5 (−/−) neurones successfully assayed with both calcium imaging and whole cell current recording to assess the effects of agonist at the low end of the concentration–response curve. *A*, calcium transients, concurrently determined with whole-cell currents, in response to 12-s applications (indicated by bars) of nicotine, cytisine, DMPP or ACh (in the presence of 0.1 μM atropine). Concentrations were 3, 5 and 10 μM (nicotine, cytisine and DMPP, respectively), and 5 and 10 μM (ACh). Sharp deviations in current traces are due to the CCD camera shutter. The experiment was conducted on a 4 DIV preparation. *B*, dose–response relationship of peak calcium transients constructed from original recordings as shown in *A*. Data are mean peak transients measured in duplicate for each agonist. Curves based on eqn (2) were simultaneously fitted to data points by unweighted non-linear regression using the Allfit routine with the constraint of a shared slope and a fixed maximum as described in Methods. Filled inverted triangles and continuous line show the concentration–response curve for cytisine (Cyt); dashed lines and open symbols are effects of DMPP (□), nicotine (Nic, ○) and ACh (◇). Potency ratios relative to cytisine (1.0) were 1.21 (DMPP), 0.74 (nicotine) and 0.37 (ACh). *C*, dose–response relationship of peak currents constructed from original recordings as shown in *A*. Data are mean peak transients measured in duplicate for each agonist. Curves based on eqn (2) were simultaneously fitted to data points by unweighted non-linear regression using the Allfit routine with the constraint of a shared slope and a fixed maximum as described in Methods. Filled inverted triangles and continuous line show the concentration–response curve for cytisine; dashed lines and open symbols are effects of DMPP (□), nicotine (○) and ACh (◇). Potency ratios relative to cytisine (1.0) were 1.49 (DMPP), 0.88 (nicotine) and 0.49 (ACh).

SCG (Kristufek *et al.* 1999). Potency ratios calculated from EC_{50} values relative to cytisine (1.0) in $\alpha5$ (+/+) mice were: DMPP, 1.61; nicotine, 1.64; Ach, 0.28. In Sprague-Dawley rats, ratios were: DMPP, 2.17; nicotine, 1.41; and Ach, 0.43 (data in rats taken from Kristufek *et al.* 1999).

Deletion of the $\alpha5$ subunit as evaluated from the transmitter release assay shifted the EC_{50} values of all agonists except of cytisine towards a higher potency (Fig. 7; Table 2). Nevertheless, potency ratios in $\alpha5$ (+/+) controls closely resembled the values of $\alpha5$ (−/−) animals (cytisine, 1; DMPP, 1.84; nicotine, 1.59; Ach, 0.47).

However, the most conspicuous effect of the deletion of the $\alpha5$ subunit was the impact it had on the efficacy of nicotinic agonists: all agonists tested stimulated a higher level of release at significantly lower doses in $\alpha5$ (−/−) compared with $\alpha5$ (+/+) animals (Fig. 7*F*). Transmitter release upon activation of prejunctional receptors was enhanced by nearly 3-fold (Fig. 7*F*).

Prejunctional nAChRs: assessment of function by low-concentration potency ratios confirms results from full concentration–response curves

Analogous to our assessment of the function of somatic nAChRs mentioned above we sought confirmation of the potency ratios calculated from EC_{50} values by applying the two most discriminating agonists, cytisine and DMPP, at low concentrations (Fig. 8). After 5 DIV, DMPP was 2.12 ± 0.16 ($n = 3$ release experiments) and 2.00 ± 0.11 ($n = 3$ release experiments) times more potent than cytisine in the $\alpha5$ (+/+) and $\alpha5$ (−/−) animals, respectively (Fig. 8). In cultures examined between 2 DIV and 8 DIV, DMPP was consistently more potent than cytisine in both $\alpha5$ (+/+) and $\alpha5$ (−/−) animals (Fig. 8*B1* and *B2*).

Age-dependent properties of SCG cultures: impact of the time *in vitro* on agonist efficacies

As mentioned above, the age of cultures had a significant impact on the relative potency of nicotinic agonists at somatic receptors in $\alpha5$ (+/+) mice (Fig. 4). However, the age of cultures also affected the overall efficacy of nicotine. Hence, in both $\alpha5$ (+/+) and $\alpha5$ (−/−) animals, the increase of intracellular calcium obtained by nicotine reached a maximum at 4 DIV and declined markedly after 7 DIV (Fig. 9*A*).

The time course of the changes in efficacy of nicotine at prejunctional receptors was determined by measuring transmitter outflow in response to a standard

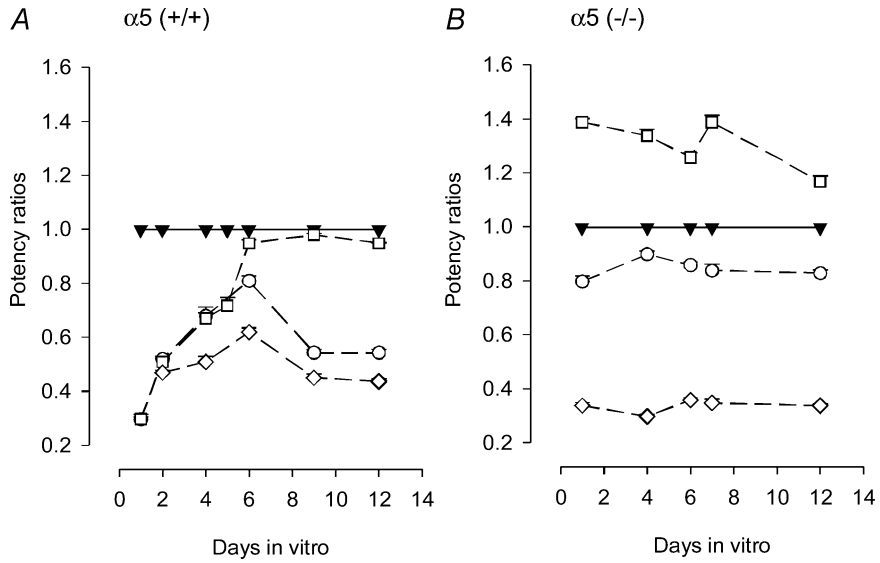

Figure 4. Time dependence of low-dose potency ratios of nicotinic agonists in $\alpha5$ (+/+) and $\alpha5$ (−/−) mice: somatic receptors

A, low-dose potency ratios were determined in individual cells from $\alpha5$ (+/+) mice at the indicated age of cultures and as shown in Fig. 2 for a cell after 4 DIV. Data points are mean potency ratios ± S.E.M. (relative to the standard, cytisine) of 6 (1 DIV), 12 (2 DIV), 21 (4 DIV), 7 (6 DIV), 2 (9 DIV) and 6 (12 DIV) neurones. Filled inverted triangles and continuous line show the potency ratio for cytisine, set to unity; dashed lines and open symbols are the ratios of DMPP (□), nicotine (○) and ACh (in the presence of 0.1 μM atropine, ◇). Note the significant change of potency ratios, particularly for DMPP, between 1 and 6 DIV ($P < 0.01$). At 1 DIV, the DMPP to cytisine ratio was 0.30 ± 0.02 ($n = 6$; significantly different from 1: $P < 0.01$), from where it increased up to 0.95 ± 0.01 ($n = 7$) after 6 DIV. *B*, results obtained from $\alpha5$ (−/−) mice by the protocol described in *A*; symbols identical to *A*. Data points are mean potency ratios ± S.E.M. (relative to the standard, cytisine) of 6 (1 DIV), 16 (4 DIV), 8 (6 DIV), 14 (7 DIV) and 8 (12 DIV) neurones. Note that regardless of the age of cultures, DMPP was consistently more potent than cytisine. At 1 DIV, the DMPP to cytisine ratio was 1.39 ± 0.01 ($n = 6$; significantly different from 1: $P < 0.01$). At 7 DIV, the DMPP to cytisine ratio was 1.37 ± 0.02 ($n = 14$).

concentration of 100 μM nicotine (in the presence of TTX) at several different DIV and for both the α5 (+/+) and α5 (−/−) genotypes (2, 5, and 8 DIV; Fig. 9*B*). As noted for somatic receptors, the efficacy of nicotine significantly declined between 5 and 8 DIV in both genotypes, and between 2 and 5 DIV in α5 (−/−) mice. The waning of the effect of nicotine between 5 and 8 DIV was not due to a general loss in the release capacity of cultures, as transmitter outflow in response to electrical field stimulation did not differ significantly either in α5 (+/+) or in α5 (−/−) mice between 5 and 8 DIV ($P > 0.05$; data not shown).

Prejunctional nAChRs: assessment of the efficacy of nicotine in the atrium preparation of α5 (+/+) and α5 (−/−) mice

We corroborated the increased efficacy of prejunctional nicotinic receptors in an acute atrium preparation taken from 6-day-old animals (Fig. 10). Transmitter release induced by a concentration of nicotine that we know caused maximal effect under conditions of action potential blockade (Figs 5 and 7) was significantly larger in α5 (−/−) compared to α5 (+/+) mice (Fig. 10). In contrast, transmitter release in response to electrical field stimulation was not affected by the genotype (Fig. 10).

Discussion

Prior studies demonstrate distinct pharmacological properties of somatic–dendritic *versus* axonally targeted nAChRs of rat SCG neurones *in vitro* (Kristufek *et al.* 1999). The current study extends these observations by initiating a systematic analysis of the potential role of nAChR subunit composition in distinct receptor pools, using mice with targeted deletions of individual nAChR subunits (for reviews see Wang *et al.* 2002*b*; Champtiaux & Changeux, 2004; Dajas-Bailador & Wonnacott, 2004). In particular, this study explores the role of α5 subunits, testing whether pharmacological differences between somato-dendritic *versus* presynaptic nAChRs may be due, at least in part, to the distinct role of the α5 subunit in nAChRs in different neuronal domains.

The simplest summary of these combined genetic and pharmacological analyses is that α5 nAChR subunits differentially contribute to nAChR pools in different cellular locales. The most intriguing and unexpected finding from our results is the *enhancement* of presynaptic nAChR-mediated NA release consequent to the deletion of α5 subunits from axonally targeted nAChRs. The implications of these findings are discussed below.

Overall, we provide three new observations regarding the profile of nAChRs expressed by mouse SCG neurones in general and the contributions of the α5 nAChR subunit in particular: (1) the pharmacological profile of somatic nAChRs depends on developmental age and on the presence or absence of α5 subunit gene expression; (2) the pharmacological profile of presynaptic nAChRs differs from that of the somatic nAChRs by being independent of developmental age and of α5 subunit gene expression; and (3) the effects of α5 deletion are most evident in changes of *presynaptic* nAChRs, implicating α5 subunits in constraining the number and/or efficacy of nAChRs linked to the presynaptic facilitation of NA release. Complementary studies in more intact (acute atrium) preparations confirm the hypothesized role of α5 subunits in shaping nicotine-evoked NA release (Fig. 10).

Contribution of α5 subunits to somatic nAChRs

Our studies revealed both age- and α5 expression-dependent differences in somatic nAChRs, including significantly higher potency of cytisine compared to DMPP at early stages (1 DIV after removal of ganglia from P4/5 mice), whereas DMPP and cytisine were essentially equipotent after 1 week *in vitro*. In contrast, in mice lacking the α5-nAChR subunit, somatic nAChRs were described by a rank order potency of DMPP > cytisine irrespective of the age of cultures. These and other data (discussed below, and see McNerney *et al.* 2000; Skok, 2002; Vincler & Eisenach, 2003; Nai *et al.* 2003) are consistent with our suggestion that mature somatic nAChRs in mouse SCG include $\alpha3\alpha5\beta4^*$ nAChRs as well as $\alpha3\alpha5\beta4\beta2^*$ nAChRs.

The rat SCG contains mRNA for α3, α5, α7, β2 and β4 (Mandelzys *et al.* 1995; De Koninck & Cooper, 1995; Zhou *et al.* 1998; D. Kristufek and S. Huck, unpublished observation). If we assume an identical subunit profile in the mouse, and if we further assume that the deletion of one subunit is not compensated by the appearance or up-regulation of another (see Kedmi *et al.* 2004), we should be able to assess the contribution of α5 to somatic nAChRs based on the differences in pharmacological profile *per se*. Elegant studies, using nAChR subunit-specific antibodies, have provided both immunohistochemical and immunoprecipitation-based evidence for the probable composition of peripheral neurone-type nAChRs in chick and human (Conroy & Berg, 1995; Wang *et al.* 1996; Gerzanich *et al.* 1998). Although comparable studies have yet to be done in rat or mouse, the prior work on other species, together with data from heterologous expression of known subunit combinations, provide important guidelines for the current study.

In the chick ciliary ganglion, most of the α5 gene product in fully assembled receptors is associated with both α3 and β4 subunits. About 20% of these receptors also contain β2 (Conroy & Berg, 1995). The first studies of α5 in heterologous recombination with other α and β subunits examined α5 plus α4 and β2 subunits from chick (Ramirez-Latorre *et al.* 1996). The $\alpha5\alpha4\beta2^*$ nAChRs had a higher conductance and a faster rate

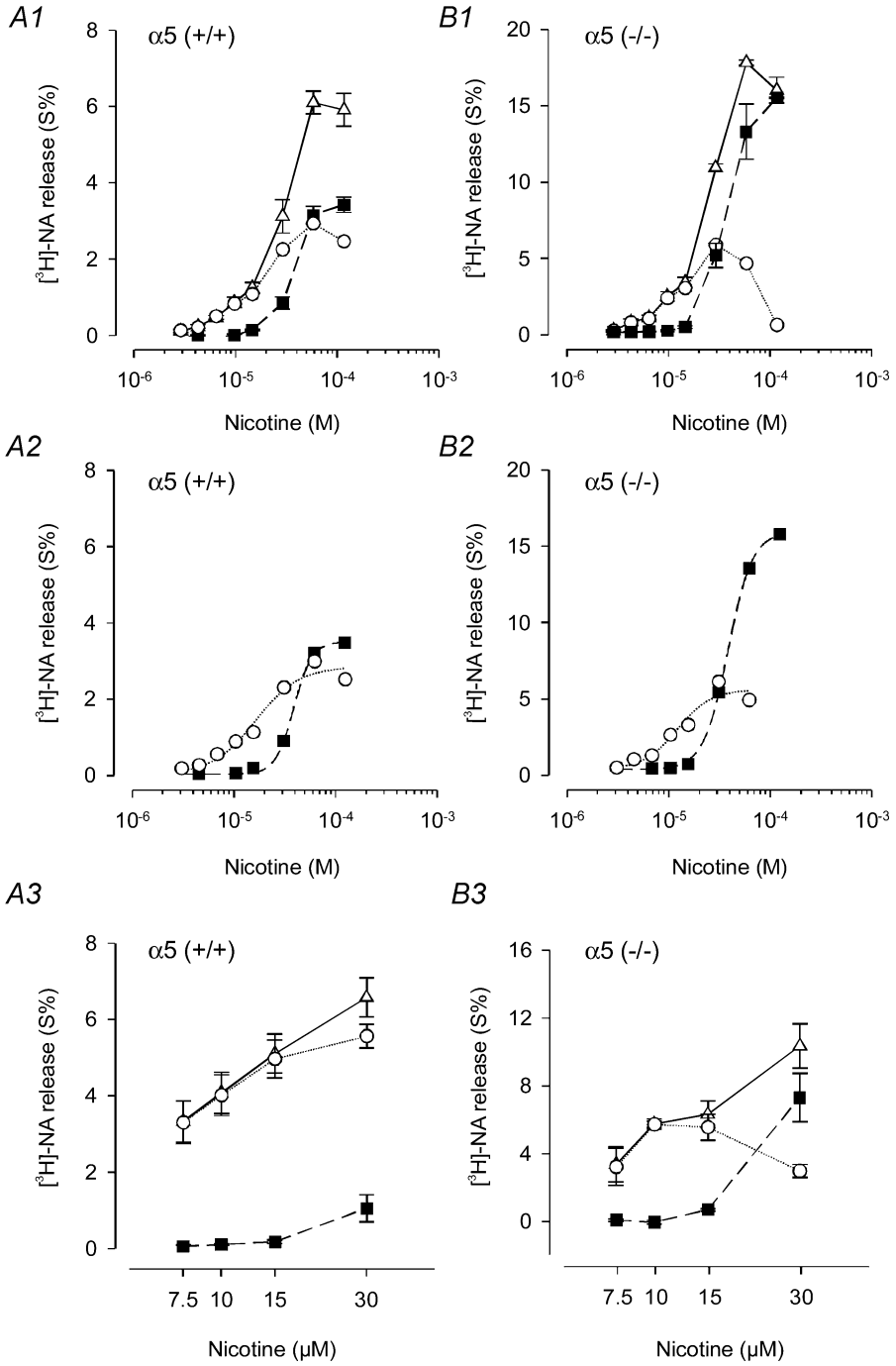

Figure 5. TTX-sensitive and TTX-insensitive transmitter release in α5 (+/+) and α5 (−/−) mice
A1, exploring full concentration–response curves in α5 (+/+) mice. Nicotine-induced transmitter release from 5 DIV SCG cultures under control conditions (overall release, △) and in the presence of 0.25 μM TTX (TTX-insensitive release, ■). Data are means ± S.E.M., $n = 3$ individual culture discs. Data points indicated by circles (TTX-sensitive release) were obtained by subtracting mean values of nicotine-induced release in the presence of TTX (■) from overall release (△). *A2*, curve fits of TTX-sensitive (○) and TTX-insensitive (■) nicotine-induced transmitter release by applying eqn (2) yielded the following parameters: EC_{50} TTX-sensitive, 15.82 ± 2.52 μM; EC_{50} TTX-insensitive, 37.46 ± 0.98 μM; maximal effect TTX-sensitive, 2.81 ± 0.22%; maximal effect TTX-insensitive, 3.47 ± 0.06%; slope factor p for TTX-sensitive, 2.03 ± 0.48; slope factor p for TTX-insensitive, 4.82 ± 0.42. Data points for the curve fits were taken from *A1*. *A3*, exploring the low concentration end of the dose–response curve. Nicotine-induced transmitter release from 2 DIV SCG cultures of α5 (+/+) mice under control conditions (overall release, △) and in the presence of 0.25 μM TTX (TTX-insensitive release, ■). Means ± S.E.M., $n = 3$ release experiments. Each data point was calculated from three triplets of individual culture discs. The data points indicated

of agonist-induced desensitization than nAChRs formed without $\alpha5$. Co-transfection of chick $\alpha5$ with $\alpha3\beta4$ in (human) BOSC 23 cells added an additional, low affinity component (EC_{50}, 512 μM) of ACh-induced currents to the higher-affinity profile (EC_{50}, 66 μM) seen with simple pairwise expression of $\alpha3$ and $\beta4$ (Fucile *et al.* 1997). These data, and our observations, are in keeping with findings in the chick SCG that functional deletion of the $\alpha5$ subunit by antisense oligonucleotide treatment removes nAChRs with relatively low affinity to ACh and cytisine (Yu & Role, 1998*b*). However, cotransfection of chick $\alpha5$ with $\alpha3\beta4$ in *Xenopus* oocytes, or of chick $\alpha5$ with $\alpha3\beta2$ in BOSC 23 cells, had little effect on either the potency or the efficacy of ACh (Fucile *et al.* 1997).

In the human neuroblastoma SH-SY5Y cell line, both $\alpha3$ and $\alpha5$ could be copurified by the $\beta2$-specific antibody mAb290, implying co-assembly of these three subunits into complexes (Wang *et al.* 1996). About 50% of $\alpha3$ receptors also contained $\beta2$ (Wang *et al.* 1996; Gerzanich *et al.* 1998). Indirect evidence suggests that $\beta4$ might substitute for $\beta2$ in the remaining receptors (Gerzanich *et al.* 1998). It is clearly pertinent to interpretation of the current study to consider how the presence of the $\alpha5$ subunit modifies combinations of $\alpha3\beta4$, $\alpha3\beta2$ and possibly $\alpha3\beta2\beta4$ human receptor subunits. This question has been addressed by co-expression of various combinations of cloned human $\alpha3$, $\beta2$, $\beta4$ and $\alpha5$ receptors in *Xenopus* oocytes (Wang *et al.* 1996; Gerzanich *et al.* 1998).

The presence of $\alpha5$ subunits increased both the rate of desensitization and the calcium permeability of receptors containing $\alpha3\beta2$ or $\alpha3\beta4$ (Gerzanich *et al.* 1998). Agonist efficacies relative to ACh were both enhanced and reduced (e.g. for nicotine or cytisine, respectively, at receptors containing $\alpha3\beta2$). Moreover, the presence of $\alpha5$ dramatically enhanced the potency of agonists at receptors including $\alpha3\beta2$, and to a lesser extent at $\alpha3\beta4$ containing receptors. Expression of all four subunits $\alpha3$, $\beta2$, $\beta4$ and $\alpha5$ resulted in complex concentration–response relations for ACh and DMPP that were fitted with the sum of two Hill equations (Gerzanich *et al.* 1998).

Overall these studies, like ours, indicate that the inclusion of $\alpha5$ subunit in nAChR complexes may selectively affect the potency and efficacy of nicotinic agonists. Depending on the age of the preparation, cytisine was either more potent than, or equipotent to, DMPP in activation of somatic receptors in wild-type (WT) mice. The deletion of $\alpha5$ reversed the potency ratios so that DMPP exceeded cytisine. The simplest interpretation of the changes we observe in somatic nAChRs with and without $\alpha5$ deletion is that $\alpha5$ is a more prominent contributor to shaping the profile of nAChRs in more mature neurones.

The differences in the agonist potency and efficacy at somatic nAChRs with/without $\alpha5$ subunits reported here, are more subtle than those seen by adding $\alpha5$ to pairwise subunit combinations of $\alpha3\beta2$ or $\alpha3\beta4$ (or even $\alpha4\beta2$) expressed in oocytes (Ramirez-Latorre *et al.* 1996; Gerzanich *et al.* 1998). This may be due to species differences (McGehee & Role, 1995), the choice of the system used to express cloned receptors (Fucile *et al.* 1997) or additional nAChR subunits that might modify the overt impact of $\alpha5$. Of particular note are the many studies

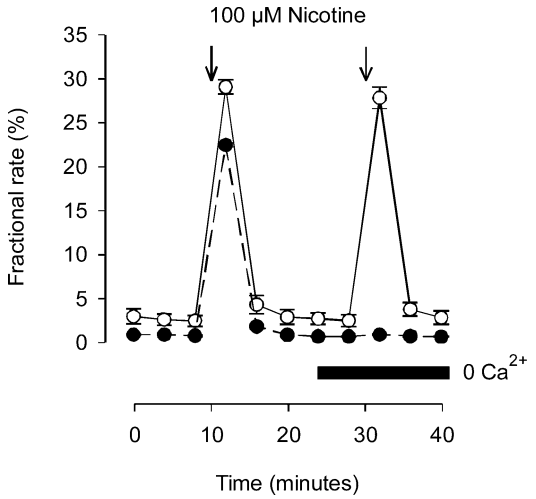

Figure 6. Calcium-dependence of TTX-insensitive transmitter release in $\alpha5$ (−/−) mice
Basal transmitter release and the release induced by 100 μM nicotine (15 s, indicated by arrows) in the presence of 0.25 μM TTX. Control buffer containing 2 mM Ca^{2+} (cultures 3 DIV, ○); superfusion buffer with and without (indicated by horizontal bar) 2 mM Ca^{2+} (cultures 2 DIV, ●). Data points are means ± S.E.M., $n = 3$.

by circles (TTX-sensitive release) were obtained by subtracting mean values of nicotine-induced release in the presence of TTX (■) from overall release (△). Note that TTX-sensitive release reached a near maximal value of 5.52 ± 0.31% ($n = 3$ cultures in triplicate) at 30 μM nicotine. *B1* and *B2,* same experimental protocols as shown in *A1* and *A2*, except that transmitter release was determined in 4 DIV cultures obtained from $\alpha5$ (−/−) mice. Fitting curves by eqn (2) to the data points shown in *B1* yielded the following parameters: EC50 TTX-sensitive, 11.71 ± 2.13 μM; EC_{50} TTX-insensitive, 37.04 ± 0.56 μM; maximal effect TTX-sensitive, 5.23 ± 0.63%; maximal effect TTX-insensitive, 15.58 ± 0.18%; slope factor p for TTX-sensitive, 2.59 ± 1.01; slope factor p for TTX-insensitive, 3.58 ± 0.15. Note that in comparison with $\alpha5$ (+/+) mice, the two preparations differ grossly in their maximal values of the TTX-insensitive component. *B3,* same experimental protocols as shown in *A3*, except that transmitter release was determined in 2 DIV cultures obtained from $\alpha5$ (−/−) mice. Note that TTX-sensitive release reached a maximum of 5.79 ± 0.19% ($n = 3$ cultures in triplicate) in response to only 10 μM nicotine (*versus* 30 μM in $\alpha5$ (+/+) mice).

suggesting that native (somatic) nAChRs are not accurately recapitulated by combinations of two or three known subunits in heterologous expression systems (Covernton *et al.* 1994; Silvilotti *et al.* 1997; Lewis *et al.* 1997).

Contribution of α5 subunits to prejunctional/preterminal nAChRs

In contrast to the apparent fine-tuning of the profile of somatic nAChRs, the current study unveiled dramatic

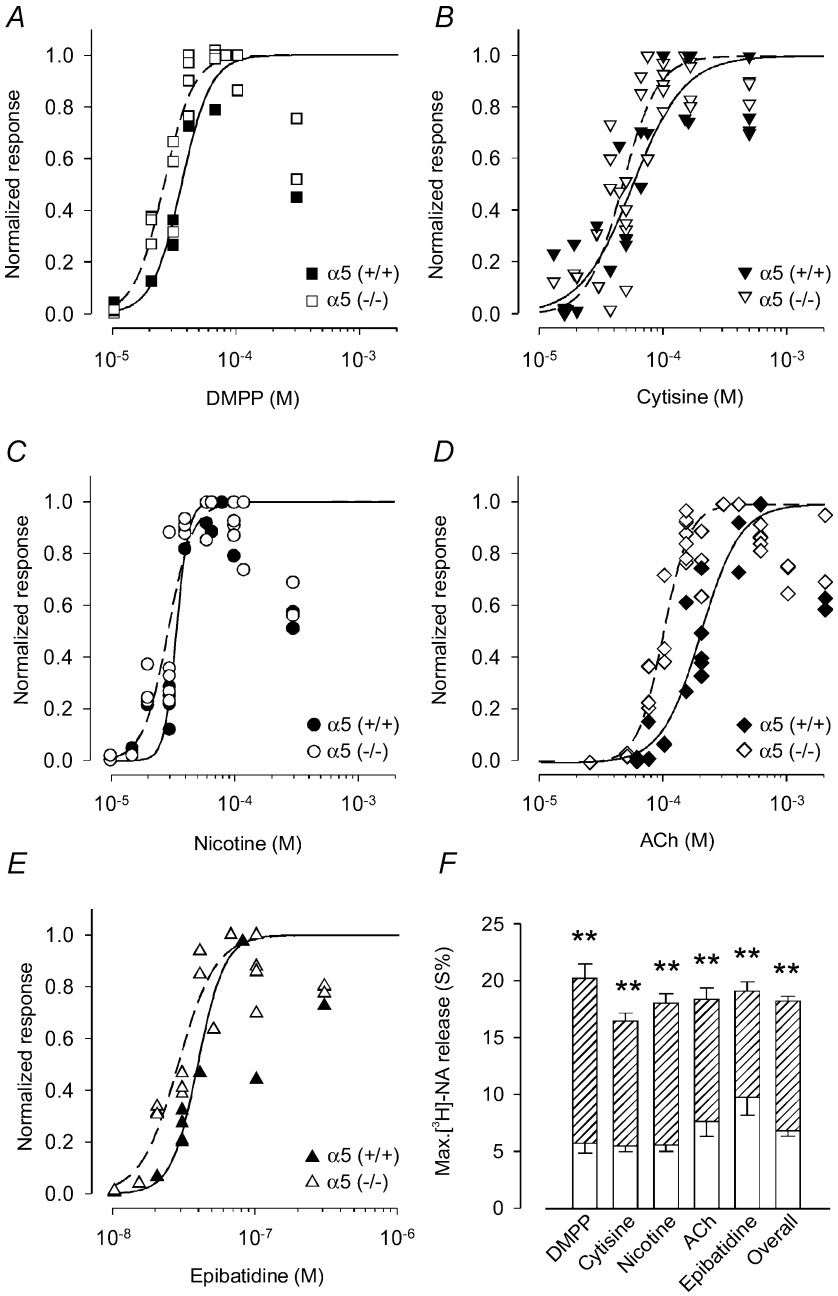

Figure 7. Transmitter release in response to activation of prejunctional nicotinic acetylcholine receptors: comparison between α5 (+/+) and α5 (−/−) mice

A–E, transmitter release overflow was evaluated in preparations at 4–6 DIV that were preloaded with [^{3}H]NA as described in Methods. Responses in the presence of 0.25 μM TTX to DMPP (*A*), cytisine (*B*), nicotine (*C*), ACh (in the presence of 0.1 μM atropine, *D*) and epibatidine (*E*) are shown. Data points show the number of counts min^{-1} of [^{3}H]NA normalized with respect to the maximum effect for each agonist in a particular experiment (DMPP, 66–100 μM; nicotine, 60–120 μM; cytisine, 75–166 μM; Ach, 150–600 μM; epibatidine, 66–100 nM) and are the averaged values from three individual cultures. Note that beyond these maximum concentrations, the effect of agonists decline again. Curves show the results of fitting eqn (2) to data points with the constraint that the maximum response was set to 1.0. Data points of supramaximal agonist concentrations were excluded from the fits. Fit parameters for EC_{50} values and the slope factors are shown in Table 2. The symbols used to depict results

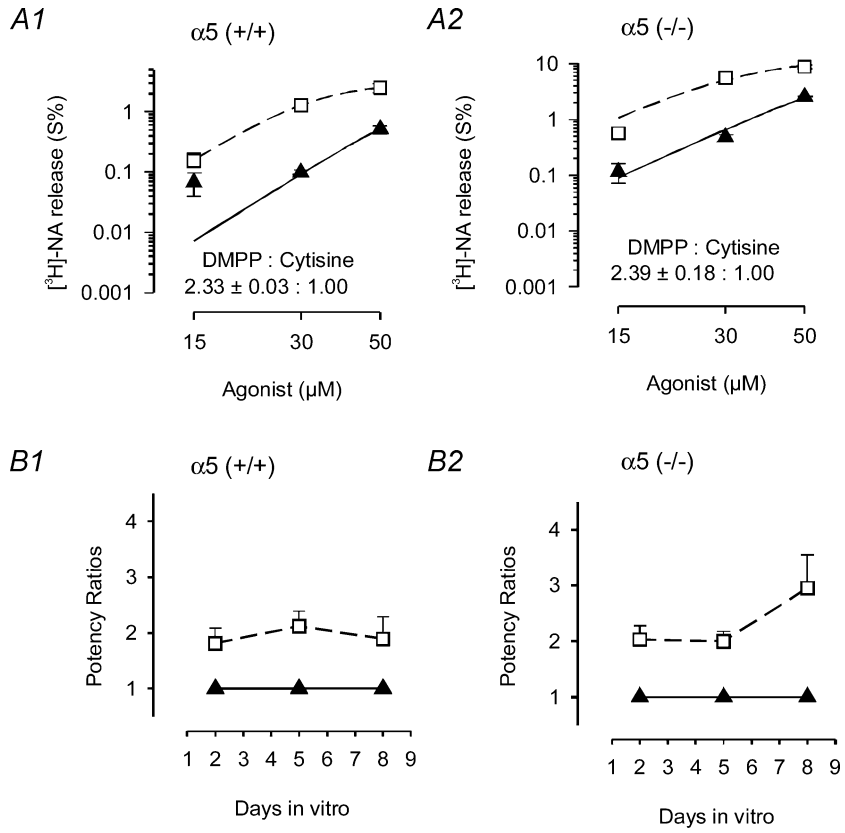

Figure 8. Agonist-induced transmitter release from α5 (+/+) and α5 (−/−) SCG cultures at low agonist concentrations

A1, transmitter release was evaluated in preparations of SCG obtained from α5 (+/+) mice at 5 DIV that were preloaded with [^{3}H]NA as described in Methods. Responses to DMPP (□) and cytisine (▲) in the presence of 0.25 μM TTX are shown. Curves based on eqn (2) were simultaneously fitted to data points by unweighted non-linear regression using the Allfit routine with the constraint of a shared slope and a fixed maximum as described in Methods. Triangles and continuous line show the concentration–response curve for cytisine; dashed line and squares are effects of DMPP. In this assay, the potency of DMPP exceeded cytisine by a factor of 2.33 ± 0.03 (n = 3 individual cultures). This experiment, done in triplicate with 5 DIV cultures, yielded a mean potency ratio of 2.12 ± 0.16 (n = 9 cultures; see *B1*). *A2*, same experimental protocol as shown in *A1*, except that transmitter release was determined in 5 DIV cultures obtained from α5 (−/−) mice. The potency of DMPP exceeded cytisine by a factor of 2.39 ± 0.12 (n = 3 individual cultures). This experiment, done in triplicate with 5 DIV cultures, yielded a mean potency ratio of 2.00 ± 0.11 (n = 9 cultures; see *B2*). *B1*, time course of potency ratios determined in preparations of SCG obtained from α5 (+/+) mice after 2, 5 and 8 DIV. For each time point, the effects of DMPP and cytisine were determined in at least three release experiments similar to the one shown in *A1*. *B2,* time course of potency ratios determined in preparations of SCG obtained from α5 (−/−) mice after 2, 5 and 8 DIV. For each time point, the effects of DMPP and cytisine were determined in at least three release experiments similar to the one shown in *A2*.

for α5 (+/+) and α5 (−/−) animals, respectively, are indicated in each panel. *F*, the maximal NA release was calculated by averaging all maximal effects an agonist had in individual cultures of either the α5 (+/+) or the α5 (−/−) genotype. Data are means ± S.E.M.; n = 9 (DMPP at α5 (+/+)) to 27 (cytisine and ACh at α5 (−/−)) individual cultures. Open columns are results from α5 (+/+) mice, hatched columns are the surplus of responses as seen in α5 (−/−) animals. Note the striking difference of the maximal release which is independent of the type of agonist ($P < 0.01$). The overall maximal NA outflow (pooled data from all five agonists) was 2.67-fold larger in α5 (−/−) than in α5 (+/+) animals (α5 (+/+), 6.82 ± 0.49%, n = 65; α5 (−/−), 18.23 ± 0.42%, n = 112; $P < 0.01$). Maximal effects of ACh in α5 (+/+) animals (7.63 ± 1.28 %; n = 15 individual cultures) did not significantly differ from the maximal effects of the other agonists ($P > 0.05$). Maximal effects of ACh in α5 (−/−) animals (18.39 ± 1.01 %; n = 27 individual cultures) did not significantly differ from the maximal effects of the other agonists ($P > 0.05$).

effects of $\alpha5$ expression (or lack thereof) on the extent of nAChR-activated (TTX-resistant) transmitter release. Such findings must be related to the plethora of prior work implicating $\alpha5$ in modulating the number, profile, rate of desensitization and calcium permeability of comparable pairwise nAChR subunit combinations (delineated above).

Indeed, measurements of somatic calcium fluxes in the $\alpha5$ (−/−) revealed slight increases compared with assays in WT mice. One might reason that even such a modest increase may be enough to support a dramatic increase in prejunctional nAChR-mediated NA release as exocytosis can follow calcium concentration to up to the fourth power (Regehr & Stevens, 2001). However, this explanation seems unlikely for three reasons. First, *all* nAChR agonists were much more effective in stimulating TTX-resistant NA release in $\alpha5$ (−/−) *versus* $\alpha5$ (+/+) animals (i.e. the increased efficacy in activation of prejunctional receptors in $\alpha5$ (−/−) mice was seen with ACh as well as other agonists). In contrast, the changes in Ca^{2+} flux at somatic receptors in $\alpha5$ (+/+) and $\alpha5$ (−/−) animals were agonist-dependent (e.g. ACh efficacy did not change). Second, even a fourth-power function of the overall increase of the somatic calcium signal ($1.14^4 = 1.69$) hardly reaches the magnitude of the observed increase in release detected in the $\alpha5$ (−/−) mice (~2.7-fold greater than $\alpha5$ (+/+)). Last but not least, our findings *vis-à-vis*

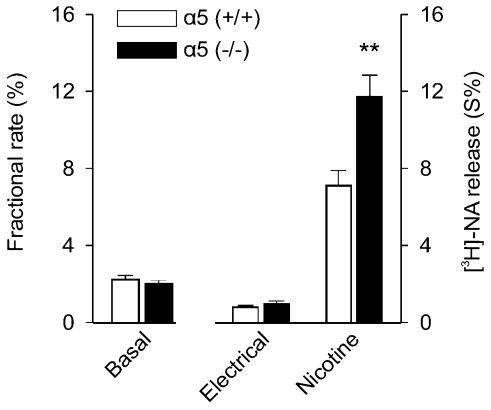

Figure 10. Transmitter release from acute mouse atrium preparations: comparison between $\alpha5$ (+/+) and $\alpha5$ (−/−) animals
Transmitter release overflow was evaluated in acute atrium preparations from 6-day-old animals upon preloading with [^{3}H]NA as described in Methods. The figure shows basal overflow, overflow induced by electrical field stimulation (120 pulses, 3 Hz), and the overflow in response to 100 μM nicotine in the presence of 0.5 μM TTX. Data points are the mean overflow ± S.E.M. from nine (wild-type) or 12 (knockout) atria. Transmitter overflow induced by nicotine was significantly larger in $\alpha5$ (−/−) compared to $\alpha5$ (+/+) animals ($P < 0.01$). Basal and electrically induced overflow did not differ significantly between preparations obtained from either knockout or wild-type animals ($P > 0.05$).

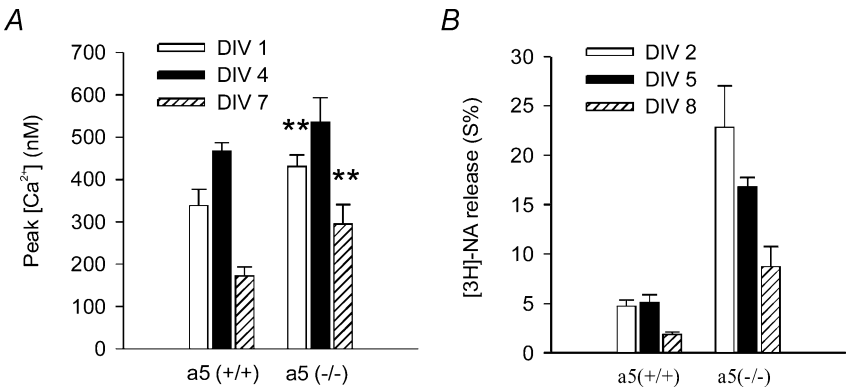

Figure 9. Time-dependence of the efficacy of nicotine at somatic and prejunctional receptors
A, somatic receptors: SCG cultures from either $\alpha5$ (+/+) or $\alpha5$ (−/−) mice were maintained for 1 DIV (open columns), 4/5 DIV (filled columns), or 7 DIV (hatched columns). Maximal effects of nicotine were determined by fitting eqn (2) to calcium transients in response to a full range of nicotine concentrations as shown in Fig. 1*F*. Note that nicotine exerted highest effects at 4/5 DIV both in $\alpha5$ (+/+) and $\alpha5$ (−/−) mice. In $\alpha5$ (+/+) mice, values at 4/5 DIV were significantly larger than at 1 DIV ($P < 0.05$) or 7 DIV ($P < 0.01$). In $\alpha5$ (−/−) mice, values at 4/5 DIV significantly exceed those at 7 DIV ($P < 0.05$). Maximal effects of nicotine were significantly larger in $\alpha5$ (−/−) than in $\alpha5$ (+/+) mice at 1 DIV and 7 DIV ($P < 0.01$). Data are means ± S.E.M., $n = 9$–27 individual cells. *B*, prejunctional receptors: transmitter release in response to 100 μM nicotine in the presence of 0.25 μM TTX. SCG cultures from either $\alpha5$ (+/+) or $\alpha5$ (−/−) mice were maintained for 2 DIV (open columns), 5 DIV (filled columns), or 8 DIV (hatched columns). Data are means ± S.E.M., $n = 24$ individual cultures (at 2 DIV), 12 (at 5 DIV) and 9 (at 8 DIV). Note that in the presence of TTX, 100 μM nicotine will cause maximal transmitter release (see Figs 5 and 7), and that at all ages, cultures obtained from $\alpha5$ (−/−) mice showed significantly more agonist-induced NA release than $\alpha5$ (+/+) animals. NA release in response to nicotine significantly declined between 5 DIV and 8 DIV both in $\alpha5$ (+/+) and $\alpha5$ (−/−) animals ($P < 0.01$), and between 2 DIV and 5 DIV in cultures taken from $\alpha5$ (−/−) mice ($P < 0.01$).

nicotine-induced changes in Ca^{2+} signals in α5 (+/+) *versus* α5 (−/−) mice appear to run contrary to predictions derived from prior studies. Thus earlier work had indicated that the exclusion of α5 would be expected to yield nAChRs of lower Ca^{2+} permeability (Gerzanich *et al.* 1998), whereas we find that genetic *removal* of α5 subunit results in the assembly of prejunctional receptors that were nearly 3-fold *more efficacious* in stimulating Ca^{2+}-dependent NA release.

We propose two possible mechanisms to explain how altering the expression of α5 nAChR subunits might regulate the extent of prejunctional nAChR-mediated NA release from sympathetic neurones: (1) α5-containing nAChRs, although somewhat higher in Ca^{2+} permeability, are less efficiently coupled to calcium-induced calcium release (CICR) from internal stores and thus less efficacious in stimulation NA release; and (2) the synthesis and incorporation of α5 into nAChRs decreases the assembly and/or insertion of non-α5-containing nAChR complexes, thus decreasing the overall number of functional nAChRs within the axon terminal domain. Arguments pertinent to these models are discussed below.

Coupling of α5 (+/+) *versus* α5 (−/−) prejunctional nAChRs to CICR and NA release

Several recent studies have emphasized the contribution of CICR to the mechanism(s) underlying the coupling of activation of presynaptic nAChRs to increased exocytosis (e.g. Shoop *et al.* 2001; Brain *et al.* 2001; Dajas-Bailador *et al.* 2002; Girod *et al.* 2003; Sharma & Vijayaraghavan, 2003; for review see Dajas-Bailador & Wonnacott, 2004). Accordingly, CICRs appear to play an important role in more sustained aspects (many minutes) of nicotine-evoked changes in Ca^{2+} signalling (for review see Dajas-Bailador & Wonnacott, 2004). As α5-containing receptors have greater rates and amounts of desensitization (e.g. Ramirez-Latorre *et al.* 1996; Gerzanich *et al.* 1998), nAChRs that do not include the α5 subunit might be more effectively coupled to enhanced release due to differences in the time course and extent of changes in local Ca^{2+} influx, and hence in CICR activation. Thus a more transient increase Ca^{2+} influx might be less effective in stimulating CICR, even if the surge in local Ca^{2+} concentration were greater in magnitude (e.g. Shoop *et al.* 2001; Brain *et al.* 2001; Dajas-Bailador *et al.* 2002; Girod *et al.* 2003; Sharma & Vijayaraghavan, 2003; for review see Dajas-Bailador & Wonnacott, 2004). However, it is not clear whether such a mechanism, though feasible, would be sufficiently different in coupling to CICR to explain the remarkable enhancement of transmitter release seen in the α5 (−/−) animals.

Role of α5 subunit gene expression in regulating the number of prejunctional nAChRs

Several investigators have underscored the effects of α5 co-expression on the overall number of functional surface nAChRs. Thus, BOSC 23 cells transfected with α3β4 show a reduction in the number of nicotine-responsive cells and of the maximum inducible current upon cotransfection with α5 (Fucile *et al.* 1997). Likewise, the number of membrane-incorporated α3β2 receptors detected by [^{125}I]mAb210 is about halved if cotransfected with α5 in *Xenopus* oocytes (Wang *et al.* 1996). According to this view the presence or absence of the α5 subunit may affect the number nAChRs on the cell surface, rather than influencing the properties of individual receptors.

One mechanism whereby increased expression of α5 subunits might be expected to decrease the number of surface nAChRs is suggested by sucrose gradient centrifugation and Western blot analysis by (Wang *et al.* 1996). These investigators suggest that the formation of α3β2α5 (and possibly α3β4α5*) nAChRs, may first require the interaction of β2 with α5 prior to the co-assembly with α3 (Wang *et al.* 1996). This process may affect the kinetics of the assembly and/or the membrane incorporation of α5-containing nAChRs. This hypothesis, like the CICR coupling concept presented above would require that somatic and prejunctional receptors are differentially affected by the expression of α5 in order to account for the observations in the present study.

In conclusion, our experiments show that deletion of the α5-nAChR subunit differentially affects somatic and prejunctional nAChRs in mouse SCG neurones. An important role of α5 subunits in determining the efficacy of nAChRs that facilitate action potential independent NA release is demonstrated. Despite these insights, we are not yet able to accurately predict the subunit composition of the nAChRs at the two different sites. However, ongoing experiments with mice lacking additional subunits, combined applications of the RNAi technique for deletion of selected subunits and immunolocalization studies with subunit-specific antibodies should soon permit identification of the α and β subunits that assemble into somatic and prejunctional receptors, respectively.

References

Boehm S & Huck S (1995). α_2-Adrenoreceptor-mediated inhibition of acetylcholine-induced noradrenaline release from rat sympathetic neurons: an action at voltage-gated Ca^{2+} channels. *Neuroscience* **69**, 221–231.

Brain KL, Trout SJ, Jackson VM, Dass N & Cunnane DC (2001). Nicotine induces calcium spikes in single nerve terminal varicosities: a role for intracellular calcium stores. *Neuroscience* **106**, 395–403.

Champtiaux N & Changeux J-P (2004). Knockout and knockin mice to investigate the role of nicotinic receptors in the central nervous system. *Prog Brain Res* **145**, 235–251.

Conroy WG & Berg DK (1995). Neurons can maintain multiple classes of nicotinic acetylcholine receptors distinguished by different subunit compositions. *J Biol Chem* **270**, 4424–4431.

Conroy WG, Liu Z, Nai Q, Coggan JS & Berg DK (2003). PDZ-containing proteins provide a functional postsynaptic scaffold for nicotinic receptors in neurons. *Neuron* **38**, 759–771.

Conroy WG, Ogden LF & Berg DK (2000). Cluster formation of α7-containing nicotinic receptors at interneuronal interfaces in cell culture. *Neuropharmacology* **39**, 2699–2705.

Covernton PJO, Kojima H, Silvilotti LG, Gibb AJ & Colquhoun D (1994). Comparison of neuronal nicotinic receptors in rat sympathetic neurones with subunit pairs expressed in *Xenopus* oocytes. *J Physiol* **481**, 27–34.

Cuevas J, Roth AL & Berg DK (2000). Two distinct classes of functional α7-containing nicotinic receptor on rat superior cervical ganglion neurons. *J Physiol* **525**, 735–746.

Dajas-Bailador FA, Mogg AJ & Wonnacott S (2002). Intracellular Ca^{2+} signals evoked by stimulation of nicotinic acetylcholine receptors in SH-SY5Y cells: contribution of voltage-operated Ca^{2+} channels and Ca^{2+} stores. *J Neurochem* **81**, 606–614.

Dajas-Bailador FA & Wonnacott S (2004). Nicotinic acetylcholine receptors and the regulation of neuronal signalling. *Trends Pharmacol Sci* **25**, 317–324.

De Koninck P & Cooper E (1995). Differential regulation of neuronal nicotinic ACh receptor subunit genes in cultured neonatal rat by sympathetic neurons: Specific induction of α5 by a Ca^{2+}/calmodulin-dependent kinase pathway. *J Neurosci* **15**, 7966–7978.

DeLean A, Munson PJ & Rodbard D (1978). Simultaneous analysis of families of sigmoidal curves: application to bioassay, radioligand assay, and physiological dose-response curves. *Am J Physiol* **235**, E97–E102.

Devay P & McGehee DS, Yu, CR & Role LW (1999). Target-specific control of nicotinic receptor expression at developing interneuronal synapses in chick. *Nat Neurosci* **2**, 528–534.

Fucile S, Barabino B, Palma E, Grassi F, Limatola C, Mileo AM, Alema S & Ballivet M (1997). α5 Subunits forms functional $\alpha3\beta4\alpha5$ nAChRs in transfected human cells. *Neuroreport* **8**, 2433–2436.

Gerzanich V, Wang F, Kuryatov A & Lindstrom J (1998). α5 Subunit alters desensitization, pharmacology, Ca^{++} permeability and Ca^{++} modulation of human neuronal α3 nicotinic receptors. *J Pharmacol Exp Ther* **286**, 311–320.

Girod R, Jareb M, Moss J & Role LW (2003). Mapping of presynaptic nicotinic acetylcholine receptors using fluorescence imaging of neurite calcium. *J Neurosci Methods* **122**, 109–122.

Groot-Kormelink PJ, Boorman JP & Silvilotti LG (2001). Formation of functional $\alpha3\beta4\alpha5$ human neuronal nicotinic receptors in *Xenopus* oocytes: a reporter mutation approach. *Br J Pharmacol.* **134**, 789–796.

Groot-Kormelink PJ, Luyten WHML, Colquhoun D & Sivilotti LG (1998). A reporter mutation approach shows incorporation of the "orphan" subunit β3 into a functional nicotinic receptor. *J Biol Chem* **273**, 15317–15320.

Grynkiewicz G, Poenie M & Tsien RY (1985). A new generation of Ca^{2+} indicators with greatly improved fluorescence properties. *J Biol Chem* **260**, 3440–3450.

Krauss KR, Carpenter DO & Kopin IJ (1970). Acetylcholine-induced release of norepinephrine in the presence of tetrodotoxin. *J Pharmacol Exp Ther* **173**, 416–421.

Kristufek D, Rudorfer W, Pifl C & Huck S (2002). Organic cation transporter (OCT) mRNA and function in the rat superior cervical ganglion. *J Physiol* **543**, 117–134.

Kedmi M, Beaudet AL & Orr-Urtreger A (2004). Mice lacking neuronal acetylcholine receptor β4-subunit and mice lacking both α5- and β4-subunits are highly resistant to nicotine-induced seizures. *Physiol Genomics* **17**, 221–229.

Kristufek D, Stocker E, Boehm S & Huck S (1999). Somatic and prejunctional nicotinic receptors in cultured rat sympathetic neurones show different agonist profiles. *J Physiol* **516**, 739–756.

Lewis TM, Harkness PC, Silvilotti LG, Colquhoun D & Millar NS (1997). The ion channel properties of rat recombinant neuronal nicotinic receptor are dependent on the host cell type. *J Physiol* **505**, 299–306.

McGehee DS & Role LW (1995). Physiological diversity of nicotinic acetylcholine receptors expressed by vertebrate neurons. *Annu Rev Physiol* **57**, 521–546.

McNerney ME, Pardi D, Pugh PC, Nai Q & Margiotta JF (2000). Expression and channel properties of α-bungarotoxin-sensitive acetylcholine receptors on chick ciliary and choroid neurons. *J Neurophysiol* **84**, 1314–1329.

Mandelzys A, De Koninck P & Cooper E (1995). Agonist and toxin sensitivities of ACh-evoked currents on neurons expressing multiple nicotinic receptor subunits. *J Neurophysiol* **74**, 1212–1221.

Nai Q, McIntosh JM & Margiotta JF (2003). Relating neuronal nicotinic acetylcholine receptor subtypes defined by subunit composition and channel function. *Mol Pharmacol* **63**, 311–324.

Nelson ME & Lindstrom J (1999). Single channel properties of human α3 AChRs: impact of β2, β4 and α5 subunits. *J Physiol* **516**, 657–678.

Nelson ME Wang F, Kuryatov A, Choi CH, Gerzanich V & Lindstrom J (2001). Functional properties of nicotinic AChRs expressed by IMR-32 neuroblastoma cells resemble those of $\alpha3\beta4$ AChRs expressed in permanently transfected HEK cells. *J Gen Physiol* **118**, 563–582.

Rae J, Cooper K, Gates P & Watsky M (1991). Low access resistance perforated patch recordings using amphotericin B. *J Neurosci Methods* **37**, 15–26.

Ramirez-Latorre J, Yu CR, Qu X, Perin F, Karlin A & Role LW (1996). Functional contributions of α5 subunit to neuronal acetylcholine receptor channels. *Nature* **380**, 347–351.

Regehr WG & Stevens CF (2001). Physiology of synaptic transmission and short-term plasticity. In *Synapses*, ed. Cowan WM, Südhof TC & Stevens CF, pp. 135–175. The Johns Hopkins University Press, Baltimore & London.

Salas R, Orr-Urtreger A, Broide RS, Beaudet A, Paylor R & De Biasi M (2003). The nicotinic acetylcholine receptor subunit α5 mediates short-term effects of nicotine in vivo. *Mol Pharmacol* **63**, 1059–1066.

Sharma G & Vijayaraghavan S (2003). Modulation of presynaptic store calcium induces release of glutamate and postsynaptic firing. *Neuron* **38**, 929–939.

Shoop RD, Chang KT, Ellisman MH & Berg DK (2001). Synaptically driven calcium transients via nicotinic receptors on somatic spines. *J Neurosci* **21**, 771–781.

Silvilotti LG, McNeil DK, Lewis TM, Nassar MA, Schoepfer R & Colquhoun D (1997). Recombinant nicotinic receptors, expressed in *Xenopus* oocytes, do not resemble native rat sympathetic ganglion receptors in single-channel behaviour. *J Physiol* **500**, 123–138.

Skok VI (2002). Nicotinic acetylcholine receptors in autonomic ganglia. *Auton Neurosci* **97**, 1–11.

Vincler MA & Eisenach JC (2003). Immunocytochemical localization of the α3, α4, α5, α7, β2, β3 and β4 nicotinic acetylcholine receptor subunits in the locus coeruleus of the rat. *Brain Res* **974**, 25–36.

Wang F, Gerzanich V, Wells GB, Anand R, Peng X, Keyser K & Lindstrom J (1996). Assembly of human neuronal nicotinic receptor α5 Subunits with α3, β2, and β4 subunits. *J Biol Chem* **271**, 17656–17665.

Wang N, Orr-Urtreger A, Chapman J, Rabinowitz R & Korczyn AD (2004). Nicotinic acetylcholine receptor α5 subunits modulate oxotremorine-induced salivation and tremor. *J Neurol Sci* **222**, 87–91.

Wang N, Orr-Urtreger A, Chapman J, Rabinowitz R, Nachmann R & Korczyn AD (2002*a*). Autonomic function in mice lacking α5 neuronal nicotinic acetylcholine receptor subunit. *J Physiol* **542**, 347–354.

Wang N, Orr-Urtreger A & Korczyn AD (2002*b*). The role of neuronal nicotinic acetylcholine receptor subunits in autonomic ganglia: lessons from knockout mice. *Prog Neurobiol* **68**, 341–360.

Williams BM, Temburni MK, Levey MS, Bertrand S, Bertrand D & Jacob MH (1998). The long internal loop of the α3 subunit targets nAChRs to subdomains within individual synapses on neurons *in vivo*. *Nat Neurosci* **1**, 557–562.

Yu CR & Role LW (1998*a*). Functional contribution of the α7 subunit to multiple subtypes of nicotinic receptors in embryonic chick sympathetic neurones. *J Physiol* **509**, 651–665.

Yu CR & Role LW (1998*b*). Functional contribution of the α5 subunit to neuronal nicotinic channels expressed by chick sympathetic ganglion neurones. *J Physiol* **509**, 667–681.

Zhou Y, Deneris E & Zigmond RE (1998). Differential regulation of levels of nicotinic receptor subunit transcripts in adult sympathetic neurons after axotomy. *J Neurobiol* **34**, 164–178.

Acknowledgements

Expert technical assistance was provided by Gabriele Koth, Andrea Motejlek and Karin Schwarz. This work was supported by grants GZ 70.072/2-PR/4/2000 (Austrian Ministry for Education, Science, and Culture to S.H.) and NS22061 (to L.W.R.).

Author's present address

H. Fischer: School of Biomedical Sciences, University of Queensland, Brisbane, QLD 4072, Australia.